https://doi.org/10.5194/egusphere-2025-4428
Preprint. Discussion started: 30 September 2025

Basic Earth Parameters from VLBI observations using Bayesian inversions in the time domain: updated insights of the Earth's interior

Yuting Cheng[1], Véronique Dehant[1,2], Attilio Rivoldini[1], Jérémy Rekier[1], and Christian Bizouard[3]

[1]Royal Observatory of Belgium, 3 Avenue Circulaire, B1180, Brussels, Belgium
[2]Université Catholique de Louvain, 1 Place de l'Université, B1348, Louvain-la-Neuve, Belgium
[3]LTE, Observatoire de Paris, 77 Avenue Denfert-Rochereau, 75014, Paris, France

Correspondence: Yuting Cheng (yuting.cheng0213@gmail.com)

Abstract. We present updated estimates of Basic Earth Parameters (BEP) from VLBI Celestial Pole Offset (CPO) time series spanning 1980-2025 using ensemble Markov Chain Monte-Carlo Bayesian inversion. Building upon Koot et al. (2008), we employ enhanced sampling algorithms and incorporate recent advances in ocean tidal modeling (Cheng and Bizouard, 2025). Key improvements include: (1) implementation of piece-wise cubic spline modeling for Free Core Nutation (FCN) amplitude variations, which significantly reduces multimodality in MCMC sampling compared to linear modeling; (2) integration of updated Ocean Tidal Angular Momentum (OTAM) values from FES2014 ocean tidal atlas (Lyard et al., 2021) without the empirical 0.7 scaling factor previously applied; and (3) utilization of five diverse CPO series from different analysis centers spanning up to 45 years of observations.

Our results show good consistency across different CPO series, with estimated dynamical ellipticity values at the edge of the 1σ range of MHB 2000. Notable findings include a larger absolute value for the imaginary part of the core-mantle boundary coupling constant ($\mathrm{Im}(K^{\mathrm{CMB}})$), approaching the 2σ boundary of Mathews et al. (2002), which may reflect contributions from multiple coupling mechanisms including topographic coupling through "form drag" effect caused by wave interactions with irregular boundaries (Rekier et al., 2025). The real part of the inner core boundary coupling constant ($\mathrm{Re}(K^{\mathrm{ICB}})$) is approximately half the MHB 2000 value, potentially indicating the need to revisit hydrostatic assumptions for the inner core given recent seismic evidence of viscous deformation. Compliance estimates suggest that frequency extrapolation methods from seismic to nutation bands require revision. The enhanced FCN free mode modeling successfully captures amplitude variations that differ from empirical models, particularly after 2000, though the physical interpretation of these differences requires further investigation.

The systematic discrepancies across multiple parameters suggest that current nutation theory needs substantial updates to incorporate more realistic models of core-mantle coupling and inner core behavior.

https://doi.org/10.5194/egusphere-2025-4428
Preprint. Discussion started: 30 September 2025

1 Introduction

Accurate knowledge of Earth orientation variations is essential for astronomy, geophysics, and space navigation applications. The Earth's rotation varies both in orientation and angular velocity because of its non-spherical shape, non-rigid and inhomogeneous interior, and the gravitational forces from celestial bodies, especially the Sun and the Moon. Developing theoretical models accurate enough to match current observational precision serves the dual purpose of enabling precise Earth orientation predictions and constraining the dynamical processes governing Earth's deep interior.

The Earth's rotation is described by a set of Earth Orientation Parameters (EOP): nutation corrections, also called Celestial Pole Offsets (CPO) with respect to a conventional model ($\mathrm{d}X$, $\mathrm{d}Y$), pole coordinates in the Earth attached reference frame (x_p, y_p) and UT1−UTC or the Length of Day (LOD). Among these rotational variations, nutation is uniquely suited for probing Earth's internal structure because the external gravitational forcing can be calculated with high precision, allowing observed deviations to be attributed to properties of Earth's interior.

These variations are continuously monitored by geodetic techniques such as Very Long Baseline Interferometry (VLBI), Global Navigation Satellite System (GNSS), Satellite Laser Ranging (SLR), and Doppler Orbitography and Radiopositioning Integrated by Satellite (DORIS). These observations are organized by dedicated international services in an operational way to maintain the realizations of the International Celestial Reference Frame (ICRF) and the International Terrestrial Reference Frame (ITRF).

Among these techniques, VLBI is the only one that uses extragalactic radio sources as reference points in the sky, which enables it to determine the orientation of the Earth in space with respect to a long-term stable reference frame and thus its variations with the longest periods - precession and nutation. VLBI uses radio telescopes far from each other on the Earth's surface to form baselines to observe simultaneously selected quasars, measuring the differences of the reception time of the wavefront at the two stations at both ends of the baseline. Geodetic VLBI observations started in the 1970s, and the precision had a major improvement in the late 1980s. The precision and network infrastructure have been continuously improving since then.

The modeling of the Earth's nutation starts from the analytical modeling of the variations caused by gravitational forces by the Sun, the Moon and the planets of the solar system acting on a rigid Earth with an ellipsoidal shape determined by the hydrodynamic equilibrium, meaning the balance between the Earth's self-gravitation and the centrifugal force of the Earth's rotation. The latest product of such modeling is REN2000 (Souchay and Kinoshita, 1996, 1997; Souchay et al., 1999). Then, transfer functions are applied to the determined amplitudes of these periodic motions to take into account the existence of the fluid outer core (FOC) and the solid inner core (SIC), coupling effects at the core-mantle boundary (CMB) and the inner core boundary (ICB), the elasticity of the Earth, and the angular momenta and loading of the fluid layer composed by the oceans and the atmosphere. Parameters related to these characteristics of the real Earth are called the Basic Earth Parameters (BEP). The current conventional nutation model, adopted by the International Astronomical Union (IAU), is MHB 2000 (Mathews et al., 2002).

https://doi.org/10.5194/egusphere-2025-4428
Preprint. Discussion started: 30 September 2025

The authors of MHB 2000 estimated some of the BEP from VLBI observations spanning from 1980 to 1999. A nutation spectrum is produced from these observations, and then the BEPs are estimated with least-squares fitting. Koot et al. (2008) estimated the same set of BEP from VLBI observations in the time domain using Bayesian inversion, estimating BEPs directly from the CPO time series observed by VLBI. Their results are mostly consistent with those of MHB 2000, except for the imaginary part of the coupling constant at the ICB ($\mathrm{Im}(K^{\mathrm{ICB}})$), which is twice in absolute value of that of MHB 2000. Zhu et al. (2017) performed estimations with both methods with VLBI observations up to 2015. They also got lager values for the same parameter despite the dataset for both methods were the same. Now that we have almost 25 years of data with better quality and also updates of global ocean models, it is time to renew such estimations to give us insights to the characteristics of the Earth's interior and interactions between the different parts of it.

In this work, we build upon the foundation established by Koot et al. (2008), employing ensemble Markov Chain Monte-Carlo (MCMC) to perform Bayesian inversion of BEP using VLBI CPO time series spanning from 1980 to 2025 (with slight variations for each series), 25 more years of better quality VLBI observations than what MHB 2000 was established on. Our analysis also benefits from the latest evaluation of ocean tidal effects on nutations (Cheng and Bizouard, 2025), where the Ocean Tidal Angular Momentum (OTAM) (Lyard & Alain, personal communication, used in Cheng and Bizouard (2025)) are derived from the FES2014 ocean tidal atlas (Lyard et al., 2021).

In the following sections, we will first present the basic structure of the inversion algorithm, focusing on FCN modeling and OTAM updates, followed by results from different CPO series and recommendations for BEP values and the new insights they provide to the Earth's deep interior.

2 Methods and model Updates

The Bayesian inversion algorithm for BEP estimation used in this work is developed by Koot et al. (2008) based on the nutation theory of MHB 2000 (Mathews et al., 1991, 2002). We provide a brief description of the structure of the algorithm here for the sake of clarity and interpretation of the results. Readers interested in more details are invited to consult the original papers.

Bayesian inversion is an algorithm based on Bayes' theorem that determines the probability distributions of parameter values using a posterior function derived from a given model (in this case, the nutation model with the set of BEP to be estimated) and observations. Unlike traditional inversion algorithms based on least-squares fitting, Bayesian inversion does not require linearization of the relationships between observables and the parameters to be estimated. We updated the sampling algorithm from a single Metropolis-Hastings sampler to an ensemble Markov Chain Monte-Carlo (MCMC) implemented by Python package "emcee". We set the number of walkers to five times the number of estimated parameters. This approach enables a more efficient and complete stochastic sampling of the probability landscape around the maximum of the posterior function.

2.1 Basics and free parameters

Since the algorithm operates in the time domain, nutation corrections are computed for each epoch in the chosen VLBI series. For each frequency term in the rigid-Earth nutation model REN 2000 (Souchay et al., 1999), the algorithm reads the

https://doi.org/10.5194/egusphere-2025-4428
Preprint. Discussion started: 30 September 2025

corresponding amplitudes and calculates transfer functions at those frequencies. These transfer functions, which incorporate the Basic Earth Parameters (BEPs), are then applied to the rigid-Earth nutation amplitudes to obtain the "real" Earth nutation amplitudes. The calculated nutation value at each epoch is formed by summing these frequency-domain contributions.

To compute residuals (observation minus calculation, O−C), the algorithm adds nutation values from the MHB 2000 model to the Celestial Pole Offset (CPO) series, then subtracts the calculated values from the current parameter set in the MCMC run. These residuals are used to evaluate the posterior probability function (see Eq. (28) of Koot et al. (2008)). Since the amplitude of the Free Core Nutation (FCN) varies with poorly understood excitations, several parameters are designated to model these variations. An additional parameter accounts for model imperfections (see Sec. 5.3 in Koot et al. (2008)). All free parameters in this setup are listed in Tab. 1.

e	dynamical ellipticity of the Earth
$e_f + \mathrm{Re}(K^{\mathrm{CMB}})$	dynamical ellipticity of the fluid core
	+ real part of the coupling constant at CMB
κ	compliance describing the deformation of the Earth under the tidal force
γ	compliance describing the deformation of the fluid core under the tidal force
$\mathrm{Im}(K^{\mathrm{CMB}})$	imaginary part of the coupling constant at CMB
$\mathrm{Re}(K^{\mathrm{ICB}})$	real part of the coupling constant at ICB
$\mathrm{Im}(K^{\mathrm{ICB}})$	imaginary part of the coupling constant at ICB
APR	real part of the amplitude of the prograde annual nutation
API	imaginary part of the amplitude of the prograde annual nutation
$\mathrm{d}\epsilon/\mathrm{d}t$	obliquity rate
c_ϵ, c_ψ	constant offsets
$tnode$	nodes for the piece-wise linear modeling of FCN amplitude
afR, afI	real and imaginary parts of FCN amplitudes at every node
σ_M	modeling imperfection

Table 1. Free parameters in the Bayesian inversion setup

2.2 Free Core Nutation modeling

The Free Core Nutation (FCN) is a rotational eigenmode of a two-layered Earth, and it can only be observed if some external force excites it. This eigenmode exists due to the offset between the rotation axis of the fluid core and the symmetry axis of the mantle and the ellipticity of the core-mantle boundary (CMB). It is retrograde (opposite to the direction of the Earth's rotation) and has a period of approximately 430 days in space. The frequency of FCN is close to diurnal in an Earth-fixed frame, so it is also called the Near Diurnal Free Wobble (NDFW). It was discovered in the 1980s thanks to the improvement of the precision of geodetic observations, thanks to the development of VLBI. The community generally acknowledges the excitation of this

https://doi.org/10.5194/egusphere-2025-4428
Preprint. Discussion started: 30 September 2025

free mode to oceanic and atmospheric loading that have close frequencies, but the nature of this excitation remains unclear, which is why FCN cannot be predicted but estimated from nutation corrections obtained by VLBI observations.

The authors of the MHB 2000 model estimated FCN using a 4-year sliding window from VLBI observations, then removed it before using the residuals to estimate BEP by doing the inversion in the frequency domain. Meanwhile, the frequency of the FCN (in cycle per mean solar day) is intrinsically related to some of the BEPs as:

$$f_{\mathrm{FCN}} = -\left(1+\frac{A_f}{A_m}\right)\left[e_f + Re(K^{\mathrm{CMB}}) - \beta + \frac{A_s}{A_f}\mathrm{Re}(K^{\mathrm{CMB}})\right]. \tag{1}$$

Therefore, such a sequential approach leaves the nutation and FCN modeling inconsistent to some extent. Koot et al. (2008) performed the inversion in the time domain, which allows FCN modeling to be integrated in the estimation of the BEPs. We build on their work and explore the integration of more sophisticated modeling of FCN within this estimation framework.

The conventional empirical FCN model is constructed by fitting a harmonic oscillation with a period of -430.21 days to CPO series observed by VLBI, using a sliding window approach to capture temporal variations in amplitude. The window length is chosen to be 7 years to demodulate FCN from the retrograde annual oscillation, and it slides every half a year (Lambert, 2007) (see https://ivsopar.obspm.fr/fcn/). We take this as a reference to compare with the amplitude variations captured by our parameterizations.

2.2.1 Piece-wise linear model

To take into account the variation with time of the amplitude of FCN, we first use a piece-wise linear model inherited from Koot et al. (2008). In addition to that, since the MCMC has more sampling capability than the Metropolis-Hasting method used by Koot et al. (2008), we leave the locations of the nodes (time points separating different pieces of the piece-wise linear function) on the timeline free to adjust, except the first and the last ones that are set to be at the beginning and the end of the VLBI CPO time series used in the inversion. Experiments show that this method has a problem of convergence for FCN-related parameters. It is easy to understand because Multiple different arrangements of node position may explain the data equally well, which inevitably leads to different plausible configuration of node positions during the sampling process of the MCMC. We try to solve this problem by running a clustering algorithm with the output samples of a first run where the node positions are free to adjust, choosing the “most frequent” combination of the node positions, and then running the MCMC for a second time with node positions fixed to this set.

2.2.2 Piece-wise cubic spline

The amplitude change between nodes in the time domain is clearly not linear. We implement a cubic spline to replace the linear function in the inversion process. Piecewise cubic spline modeling does not increase the dimension of the parameter space, yet it enables the capture of the continuous and non-linear changes in the amplitude of FCN, allowing the positions of the nodes on the timeline to be free to adjust in the MCMC run, ensuring the consistency of this FCN model with the reset of BEP.

https://doi.org/10.5194/egusphere-2025-4428
Preprint. Discussion started: 30 September 2025

The result shows this modification significantly reduces the multimodality of the FCN-related parameters during MCMC sampling, to an extent that clustering and rerunning are no longer necessary. We will discuss these details of the results in the dedicated section.

2.3 OTAM from FES 2014

Ocean tidal effects account for a significant portion of the nutation perturbations due to the non-rigidity of the Earth. It is particularly important for the determination of normal modes of the Earth in the presence of the fluid outer core and the solid inner core. These effects can be calculated from Ocean Tidal Angular Momentum (OTAM) calculated from a global ocean tidal model. The OTAM values used in MHB 2000 is from Chao et al. (1996), and they applied an independent constant scaling factor of 0.7 to take into account the inaccuracy of OTAM ocean tidal maps. They pointed out that this inaccuracy comes essentially from the calculation of the current angular momentum of which the large contributions usually come from small but deep oceanic area. Cheng and Bizouard (2025) calculated effects of major tidal terms on nutation separately and reported significant differences comparing to those of the MHB 2000 nutation model (see Tab. 2). These differences come mainly from the update of ocean tide maps, and the contribution from the differences in the transfer function is not significant. Cheng and Bizouard (2025) found good correlations between tidal amplitudes estimated from different CPO series and their modeled values, but with observed amplitudes being only about 30% of the modeled values. This suggests that the 0.7 scaling factor applied in the MHB 2000 model to reduce ocean tidal effects may have been unnecessary.

In this study, We updated the OTAM values with those calculated from the FES 2014 ocean tidal atlas (Lyard & Alain, personal communication, used in Cheng and Bizouard (2025)), and kept the same dynamic equations and admittance interpolations without the scaling factor. Note that comparing to MHB 2000, the J_1 tide is now also part of the main waves derived from the ocean tide map and contributes to the determination of the interpolation function.

tidal term	Doodson	celestial period	dA_{re} (μas)	dA_{im} (μas)
K_1^+	165.565	−6794.03	−52	−36
ψ_1	166.554	−365.25	101	−109
ϕ_1	167.555	−182.62	11	−7
O_{O_1}	185.555	−13.66	3	−3
O_1	145.555	13.66	−12	40
P_1	163.555	182.62	42	16
S_1	164.556	365.24	33	2
-	165.545	6802.63	8	4

Table 2. Differences of amplitudes of typical ocean tidal terms (BCFES2014-MHB2000) from Cheng and Bizouard (2025)

https://doi.org/10.5194/egusphere-2025-4428
Preprint. Discussion started: 30 September 2025

Table 3. Matter (ma) and motion (mo) terms of the equatorial ocean angular momentum raised by the ocean tides according to FES 2014 model (Lyard & Alain, personal communication). Amplitude (h_x^σ, h_y^σ) in unit of 10^{24} kg m^2 s^{-1}, phase $(\phi_x^\sigma, \phi_y^\sigma)$ in degrees.

	x		y		x		y	
	h_x^{ma}	ϕ_x^{ma}	h_y^{ma}	ϕ_y^{ma}	h_x^{mo}	ϕ_x^{mo}	h_y^{mo}	ϕ_y^{mo}
Q_1	1.0975	−19.8513	2.6944	−145.0860	0.6306	−58.4403	0.6926	−150.3420
O_1	4.4929	−32.6149	11.9198	−137.1860	3.1332	−58.0996	4.4857	−159.0040
P_1	1.5891	−50.7169	4.4485	−133.3250	1.7432	−66.7756	2.5541	−166.2160
S_1	0.2080	−176.7470	0.2804	−72.0892	0.1636	−46.3669	0.2312	168.7660
K_1	4.8055	−52.7426	13.2476	−132.7600	5.4472	−66.2532	8.0517	−166.6610
J_1	0.2941	−58.1420	0.7580	−132.9610	0.1778	−62.8905	0.4420	179.5610

Solution name	Processing software	Time span	Mean STD (mas)
ivs24q4X.eops	DOGSC_CS	1984.06 - 2024.96	0.54
vie2023a.eoxy	VieVS	1980.73 - 2025.17	0.11
usn2024b.eoxy	Calc/nμSolve	1980.28 - 2025.20	0.14
gsf2023a.eoxy	Calc/nμSolve	1980.28 - 2025.17	0.11
gfz2022a.eoxy	PORT	1980.28 - 2022.99	0.34

Table 4. CPO series used in this study

3 Results and discussions

We used most of the up-to-date CPO series from different analysis centers that use different software for post-processing. They are listed in Tab. 4. They are provided by the International VLBI Service for Geodesy and Astrometry (IVS; Nothnagel et al. (2017)) and archived at NASA's Crustal Dynamics Data Information System (CDDIS; Noll (2010)). Note that the ivs24q4X series is a solution-level combination of series from different analysis centers adopted by the International VLBI Services (IVS) combination center.

3.1 Methodological Improvements and Their Impact on BEP Estimation

We demonstrate the effects of our methodological enhancements using the usn2024b CPO series as a representative example. Two improvements are examined: the implementation of updated Ocean Tidal Angular Momentum (OTAM) corrections and the adoption of piece-wise cubic spline modeling for FCN amplitude variations.

We replaced the OTAM values from Chao et al. (1996) with those derived from the FES2014 ocean tidal atlas(Lyard et al., 2021), removing the empirical 0.7 scaling factor applied in MHB 2000. The updated OTAM values show significant differences from the original model, particularly for major tidal terms (see Tab. 2). These changes propagate through the transfer function calculations and directly impact the estimated BEPs, especially the compliances (κ and γ) and coupling constants (K^{CMB} and

https://doi.org/10.5194/egusphere-2025-4428
Preprint. Discussion started: 30 September 2025

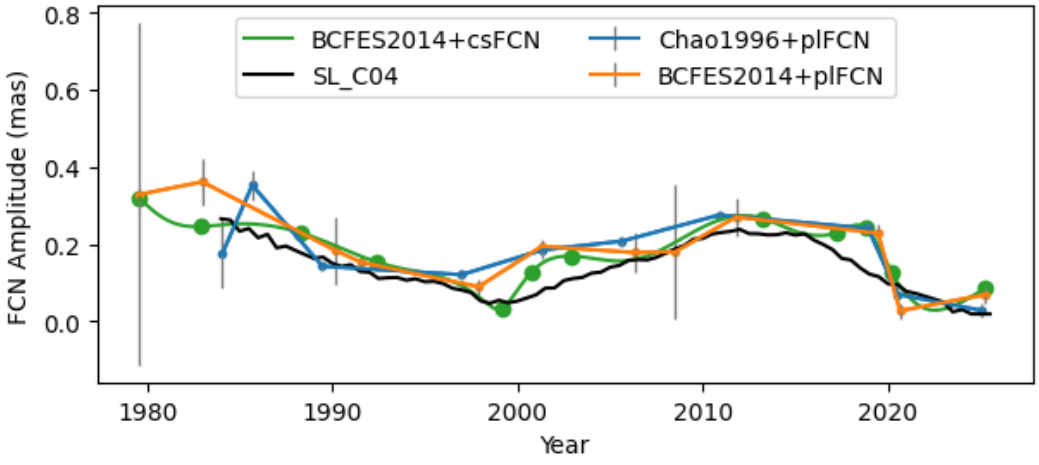

Figure 1. Amplitude variations of the Free Core Nutation (FCN) from usn2024b, with different OTAM values (from Chao et al. (1996)) and 'BCFES2014' (Cheng and Bizouard, 2025) and different modeling of FCN amplitudes ('pl' for piece-wise linear and 'cs' for piece-wise cubic spline), compared with the empirical model fitted with a sliding window (Lambert, 2007)(in black).

K^{ICB}) as shown in Fig.2. Note that in our solution when we use OTAM values from Chao et al. (1996), the scale factor of 0.7 was not applied.

We can see in Fig. 1 that the use of cubic splines affects the choice of node positions and better captures the amplitude variations of FCN. It is in general very close to the empirical model (Lambert, 2007), but we notice some differences, especially after 2000. Fig.3 shows FCN amplitudes from all used series with piece-wise cubic spline modeling with 12 nodes. They are in good agreement, which confirms their differences with the empirical model after 2000.

The differences between piece-wise linear and cubic spline modeling of FCN amplitudes can be seen in the coupling constants, not only the one that is directly related to the FCN frequency (K^{CMB}), but also K^{ICB}, which is related to the inner core coupling and the frequency of FICN.

Finally, Fig. 4 shows the distributions of BEP from all series with a piece-wise cubic spline modeling with 12 nodes, and the corresponding estimated values and their standard deviations are listed in Tab. 5. We will go through them in the following session.

3.2 Geophysical interpretaions

3.2.1 Dynamical ellipticities and the core-mantle coupling

The estimated dynamical ellipticity e of all series are in good agreement, locating at the edge of 1σ range of the MHB 2000 value. This parameter is related to the precession rate, which is correlated with the 18.6-year nutation. The CPO series we have used cover about two periods of the 18.6-year nutation.

https://doi.org/10.5194/egusphere-2025-4428
Preprint. Discussion started: 30 September 2025

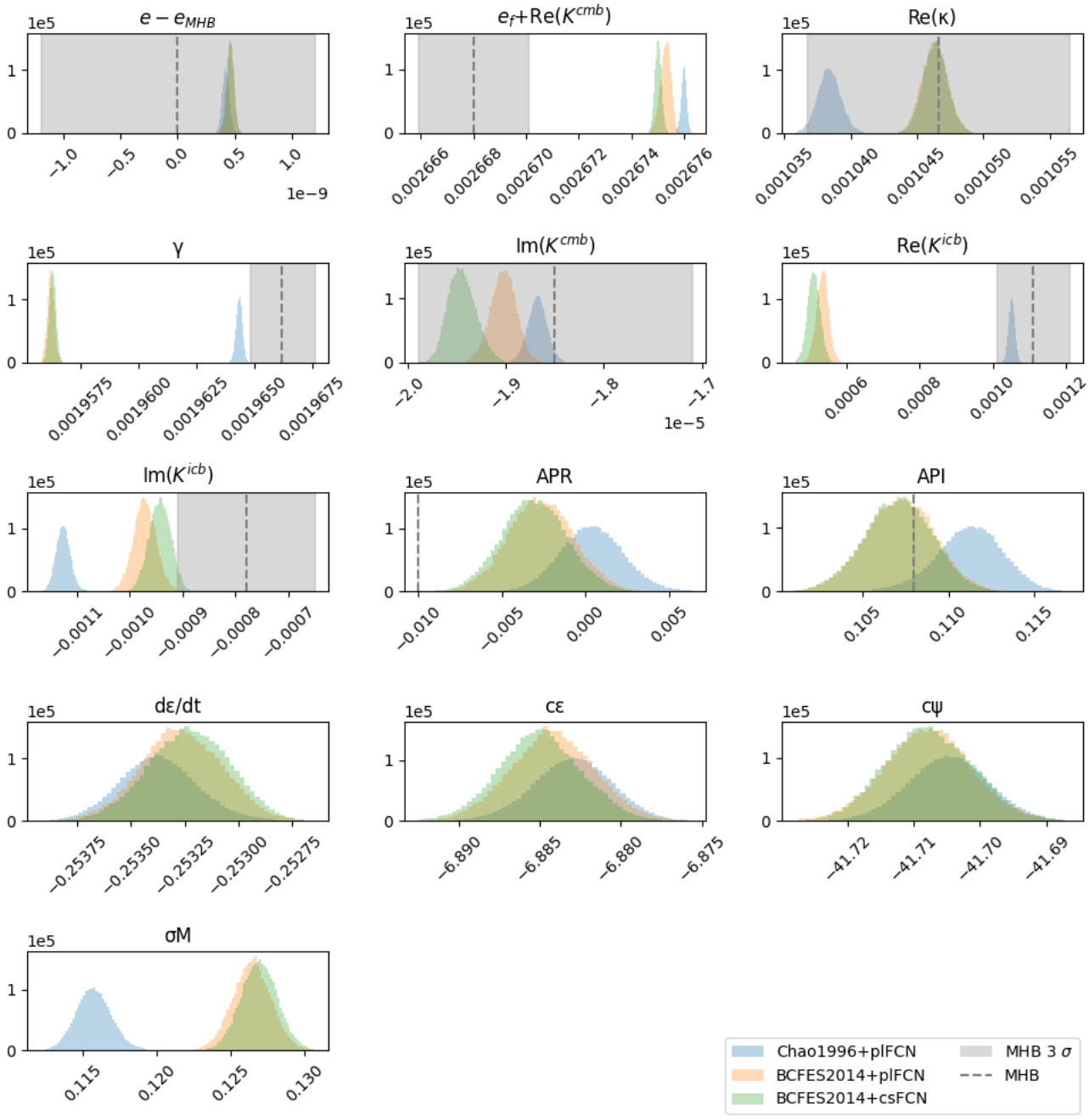

Figure 2. Distributions of BEP from usn2024b, with different OTAM values (from Chao et al. (1996)) and 'BCFES2014'(Cheng and Bizouard, 2025) and different modeling of FCN amplitudes ('pl' for piece-wise linear and 'cs' for piece-wise cubic spline), compared with MHB 2000 values (black lines) and 3 σ ranges (grey areas). $e_{\text{MHB 2000}} = 0.0032845479$.

https://doi.org/10.5194/egusphere-2025-4428
Preprint. Discussion started: 30 September 2025

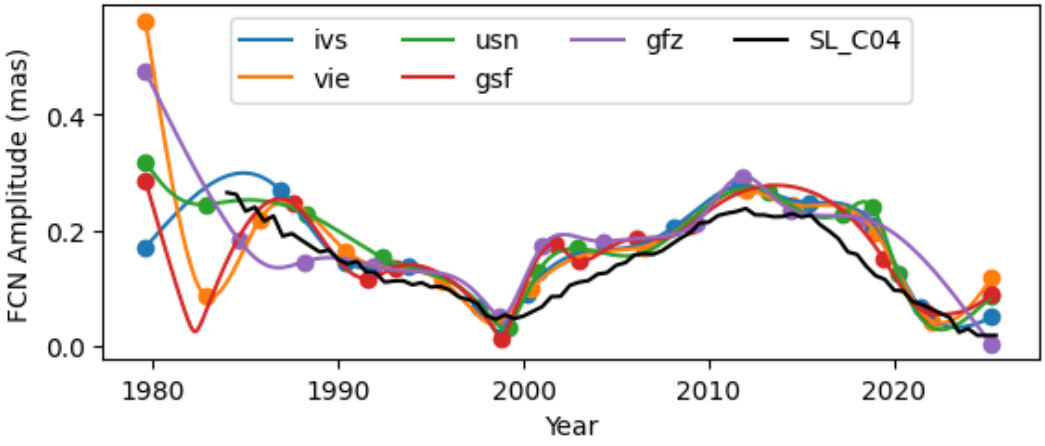

Figure 3. Amplitude variations of the Free Core Nutation (FCN) from all series, compared with the empirical model (in black). In these cases, the variations are modeled as piece-wise cubic splines with 12 nodes (marked with dots) for each series.

The dynamical ellipticity of the FOC (e_f), the real part of the coupling constant at CMB (Re(K^{CMB})), and the compliance β cannot be estimated independently, as they appear as a linear combination in the FCN frequency expression (see Eq. 1). The estimation of $e_f + \mathrm{Re}(K^{\mathrm{CMB}}) - \beta$ is significantly larger than the MHB 2000 value. The compliance β is fixed to the value calculated from PREM since it is the parameter of which the theoretical value has the smallest uncertainty. The departure of β from this value (the real part) can be considered included in this term. A reevaluation and numerical separation of these correlated parameters will need careful consideration from a theoretical point of view.

More notably, the estimated imaginary part of K^{CMB} has a larger absolute value than MHB 2000, approaching the 2σ boundary. Following the relationship illustrated in Fig. 1 of Mathews et al. (2002) (see also Fig. 2 of Buffett et al. (2002)), this would require an RMS radial magnetic field of approximately 0.75 mT to account for this observation through electromagnetic coupling alone. Such a field strength would necessitate unrealistically high and uniform conductivity throughout the lower mantle (Rekier et al., 2025; Lobanov et al., 2021). Recent work by Rekier et al. (2025) proposes an alternative mechanism involving topographic coupling from drag theory and internal wave excitation at the CMB, which could explain the observed dissipation without requiring implausibly high lower mantle conductivity. The larger Im(K^{CMB}) values we observe may thus reflect contributions from multiple coupling mechanisms rather than purely electromagnetic effects.

This makes it hard to interpret our estimation of e_f, since the contribution of electromagnetic coupling to Re(K^{CMB}) is uncertain. We can nevertheless give some constraints considering different scenarios. Mathews et al. (1991) estimated that the e_f exceeds the hydrostatic value ($e_f[\mathrm{hydrostatic}] = 0.002548$) of about 3.8%, which corresponds to an increase of the core equatorial radius of 370 m. From our estimations, if $\mathrm{Re}(K^{\mathrm{CMB}}) = 0$, e_f increases about 4.9% comparing to the hydrostatic value. If we attribute all observed Im(K^{CMB}) to electromagnetic coupling, leading to $\mathrm{Re}(K^{\mathrm{CMB}}) \approx 2.5 \times 10^{-5}$, then e_f increases

https://doi.org/10.5194/egusphere-2025-4428
Preprint. Discussion started: 30 September 2025

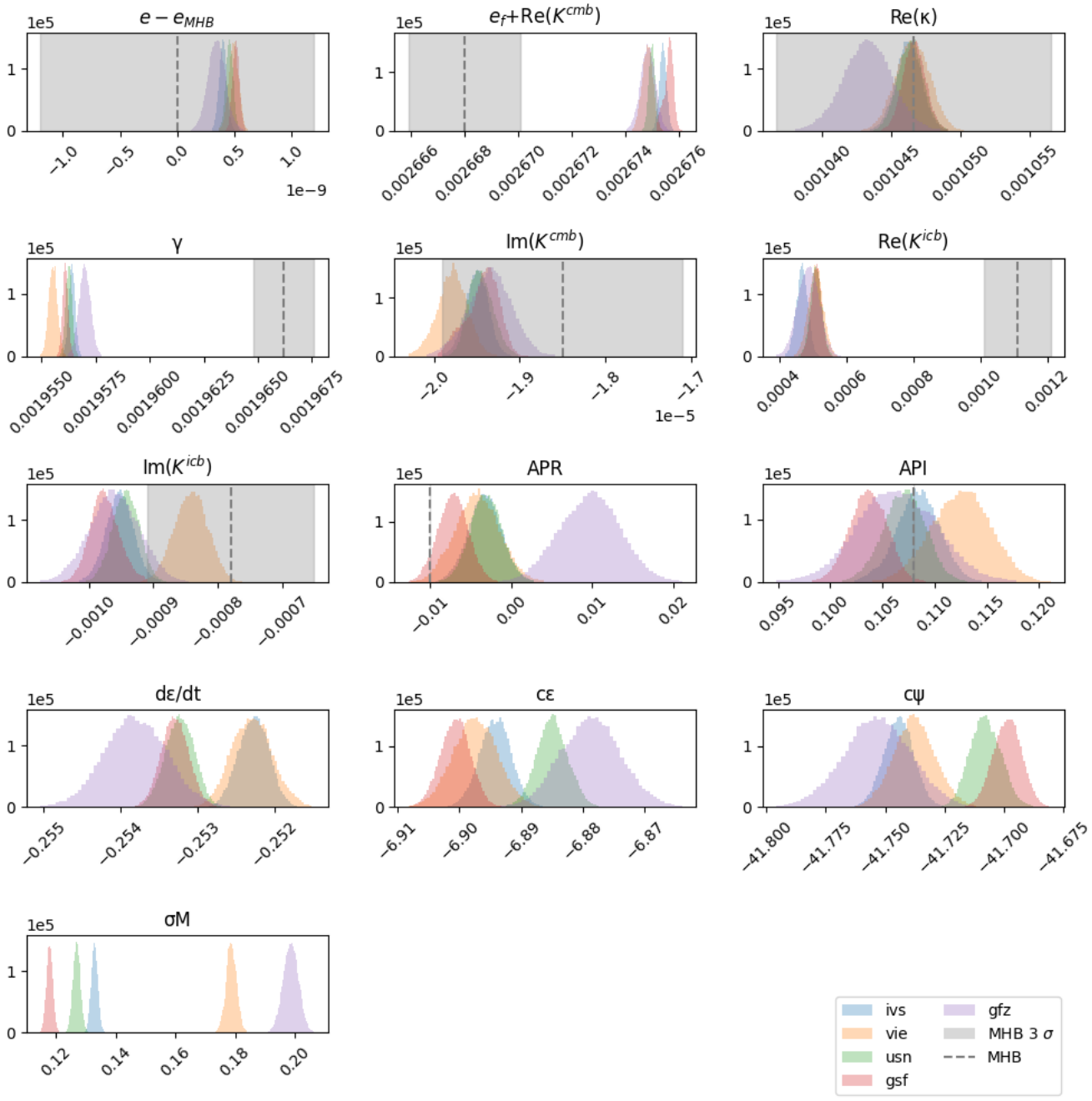

Figure 4. Distributions of BEP from all series, compared with MHB 2000 values (black lines) and 3 σ ranges (grey areas). FCN amplitudes in these cases are modeled as piece-wise cubic splines with 12 nodes (see Fig.3). $e_{\mathrm{MHB\ 2000}} = 0.0032845479$.

https://doi.org/10.5194/egusphere-2025-4428
Preprint. Discussion started: 30 September 2025

	ivs24q4X	vie2023a	usn2024b	gsf2023a	gfz2022a	MHB 2000
$e - e_{\text{MHB 2000}}$	4.0	4.9	4.6	5.2	3.5	-
(10^{-10})	±0.3	±0.4	±0.3	±0.3	±0.8	±4
$e_f + \text{Re}(K^{\text{CMB}})$	0.00267541	0.00267483	0.00267501	0.00267562	0.00267485	0.0026680
	±0.00000013	±0.00000019	±0.00000012	±0.00000018	±0.00000027	±0.0000007
κ	0.00104624	0.00104655	0.00104639	0.00104666	0.00104327	0.0010466
	±0.00000093	±0.0000012	±0.00000091	±0.00000081	±0.00000018	±0.00000033
γ	0.00195641	0.00195553	0.00195627	0.00195610	0.00195700	0.00196620
	±0.00000015	±0.00000020	±0.00000014	±0.00000013	±0.00000027	±0.00000046
$\text{Im}(K^{\text{CMB}})$	−0.00001950	−0.00001978	−0.00001944	−0.00001943	−0.00001934	−0.00001850
	±0.00000013	±0.00000018	±0.00000014	±0.00000019	±0.00000025	±0.00000046
$\text{Re}(K^{\text{ICB}})$	0.000467	0.000509	0.000509	0.000510	0.000487	0.00111
	±0.000017	±0.000022	±0.000017	±0.000016	±0.000031	±0.000033
$\text{Im}(K^{\text{ICB}})$	−0.000952	−0.000841	−0.000943	−0.000975	−0.000961	−0.00078
	±0.000021	±0.000026	±0.000020	±0.000023	±0.000038	±0.000043
APR (mas)	−0.003	−0.004	−0.003	−0.007	0.010	−0.01
	±0.002	±0.003	±0.002	±0.002	±0.004	-
API (mas)	0.108	0.112	0.107	0.104	0.106	0.108
	±0.002	±0.003	±0.002	±0.002	±0.004	-
$\text{d}\epsilon/\text{d}t$ (mas/y)	−0.2523	−0.2523	−0.2532	−0.2533	−0.2538	−0.237*
	±0.0002	0.0003	±0.0002	±0.0002	±0.0004	±0.003*
c_ϵ (mas)	−6.892	−6.897	−6.885	−6.901	−6.879	-
	±0.003	±0.004	±0.003	±0.002	±0.005	-
c_ψ (mas)	−41.744	−41.737	−41.708	−41.698	−41.753	-
	±0.006	±0.009	±0.007	±0.006	±0.014	-
σ_M (mas)	0.132	0.179	0.127	0.12	0.20	-
	±0.001	±0.002	±0.001	±0.001	±0.003	-

Table 5. Estimated BEP with standard deviation from all used CPO series, applying BCFES2014 OTAM and using piece-wise cubic spline with 12 nodes for FCN modeling. Values from MHB 2000 are listed in the last column for comparison. Also see histograms in Fig.4. *Note that the MHB 2000 value of $\text{d}\epsilon/\text{d}\psi$ comes from Herring et al. (2002) where the obliquity rate ($\text{d}\epsilon/\text{d}\psi$) and constant offsets ($c_\epsilon$ and c_ψ) are estimated with amplitudes of 21 nutation terms, while the values of constant offsets are not given. $e_{\text{MHB 2000}} = 0.0032845479$.

about 4.0% comparing to the hydrostatic value. In any case, we would have a non-hydrostatic contribution between 370 m and 500 m in terms of core equatorial radius increase.

3.2.2 The inner core

Our estimation of $\text{Re}(K^{\text{ICB}})$ appears to be almost half of the MHB 2000 value. This parameter is related to the Free Inner Core Nutation (FICN) frequency (in cycle per mean solar day) as:

$$\sigma_{FICN} \simeq -1 + \alpha_2 e_s + \nu - K^{\text{ICB}} \tag{2}$$

Similar to $\text{Re}(K^{\text{CMB}})$, it appears as a linear combination with $\alpha_2 e_s$, e_s being the inner core ellipticity, α_2 approximately a combination of the density jump at the ICB, the outer core density, and the inner core density, and K^{ICB} the coupling constant at the ICB. In our inversion setup, the values of e_s and α_2 are fixed to PREM values with the assumption that the inner core

https://doi.org/10.5194/egusphere-2025-4428
Preprint. Discussion started: 30 September 2025

boundary corresponds to the surface of hydrostatic equilibrium, which was supported by studies in late 90s, evaluating dynamic topographies associated with the existence of mass anomalies in the inner core and in the mantle, to be below 100m (Defraigne et al., 1996). Note that the compliance ν is also fixed to the value calculated from PREM for the same reason as β. Considering electromagnetic coupling only, our value would require a magnetic field at the ICB lower than MHB 2000 and thus closer to geodynamo results (between 10 and 40 Gauss [0.1-0.4 T] (Aubert, 2013). Recent studies by Wang et al. (2024); Vidale et al. (2025) revealed from seismic data possible viscous deformation at the inner core boundary (ICB) occurring on timescales of years. The hydrostatic assumption of the inner core in nutation computations could thus be revised. In addition, the density jump at the ICB could also be revised in view of the possible evidence of a mushy zone at the ICB (Tian and Wen, 2017).

Moreover, our estimation of the imaginary part of K^{ICB} is slightly larger in absolute value comparing to MHB 2000, which is, in a way, contradictory to the results of the real part considering the relation given by Fig. 2 in Mathews et al. (2002) (see also Fig. 2 of Buffett et al. (2002)) by electromagnetic coupling at the ICB.

3.2.3 Compliances

Compliances describe the deformability of the Earth (or different parts of it) under certain forcing. The two compliances in our free parameter set are κ, describing the deformability of the whole Earth under tidal force, and γ, describing the deformability of the fluid core under tidal force. Our estimation of κ is in complete agreement with MHB 2000, while our estimated value of γ is significantly smaller than that of MHB 2000.

These compliances reflect the anelasticity of Earth's interior, which is frequency dependent. PREM (Dziewonski and Anderson, 1981) used high-frequency seismic data (with periods from several seconds to one hour) to estimate the Earth rheological properties from which these compliances are determined, then extrapolated these values to the nutation band (diurnal frequencies) using power-law scaling with frequency ratios. However, the exponent of this power-law scaling is poorly constrained. While estimated values in MHB 2000 were consistent with theoretical values derived through this extrapolation method, this is no longer the case with our results. The γ value that we obtained indicates a less deformable fluid core, from which we conclude that the frequency extrapolation method itself may require revision when considering the deformation at the CMB.

3.2.4 Corrections to the prograde annual terms

The atmosphere contributes to nutation mainly in the prograde and retrograde annual, semi-annual, and ter-annual frequencies. There is as well a contribution to the retrograde annual nutation due to the resonance effect to the FCN. Evaluating these effects using atmospheric angular momentum (AAM) data remains non-trivial, as it requires data with a high sampling rate to capture the quasi-diurnal effects in a frame tied to the Earth. The largest effect is at the prograde annual nutation. Therefore, a prograde annual term is included in the estimated parameters to account for this atmospheric effect as it is the most important contribution (Yseboodt et al., 2002). The results of our estimations of this term vary about 20 μas between different solutions from different IVS analysis centers. It should be noted that this prograde annual term is empirical and will absorb not only the atmospheric contribution but also any other signals appearing in VLBI observations as prograde annual oscillations, which are typically associated with Earth's revolution around the Sun and the resulting annual temperature variations.

https://doi.org/10.5194/egusphere-2025-4428
Preprint. Discussion started: 30 September 2025

Two CPO series are generated using Calc/nμSolve to test the effect of different mapping functions of the tropospheric delay in VLBI data processing. The considered mapping functions are VMF1 (re3data.org, 2020) and NMF (Niell, 1996). The resulting differences appear primarily in the prograde annual term at the level of 2 μas, which corresponds to the uncertainty of this parameter in individual data series. The differences on K^{CMB} and K^{ICB} are not significant.

3.2.5 Additional parameters

We have considered the same set of additional parameters that are adjusted at the same time with geophysical parameters as in Koot et al. (2008): the obliquity rate $\mathrm{d}\epsilon/\mathrm{d}t$, constant offsets c_ψ and c_ϵ, and the modeling uncertainty σ_M. Their presence in MHB 2000 is not obvious, but they were actually evaluated by Herring et al. (2002) before the final BEP estimations for MHB 2000 by Mathews et al. (2002).

The obliquity rate $\mathrm{d}\epsilon/\mathrm{d}t$ was estimated together with 21 nutation frequencies by Herring et al. (2002). Their result is also included in Tab. 5. Herring et al. (2002) also estimated the secular obliquity change with nutation amplitudes fixed to MHB 2000 values, where they found $\mathrm{d}\epsilon/\mathrm{d}t = -0.252 \pm 0.003$ mas/yr, which is closer to our result. Note that the FCN is also estimated in both cases with its time-varying amplitude represented as piece-wise linear functions, with 6 and 10 nodes for time series spanning about 20 year. However, their results of the constant offsets c_ψ and c_ϵ are not given.

The parameter σ_M introduced by Koot et al. (2008) incorporates both the modeling error and a constant correction to the standard deviation of the data (see Eq. (28) in Koot et al. (2008)). Standard deviations are used to represent the uncertainties of CPO estimated from VLBI observations, but they are usually smaller than the real uncertainties. With σ_M, this possibility of underestimation of CPO uncertainties is taken into account. It thus partially has the same goal as the parameter introduced by Herring et al. (2002) to correct data errors.

4 Concluding remarks

This study presents an updated estimation of Basic Earth Parameters from VLBI observations by Bayesian inversion, incorporating 25 additional years of higher-quality data compared to the conventional nutation model MHB 2000 (Mathews et al., 2002; Herring et al., 2002; Buffett et al., 2002). Our enhanced methodology, incorporating ensemble MCMC sampling, piece-wise cubic spline FCN amplitude modeling, and updated OTAM corrections, provides robust parameter estimates with improved precision.

The consistency of results across five CPO series from different analysis centers using different post-processing software validates our approach and strengthens confidence in the estimated values. These estimations give us new geophysical insights, including evidence for multiple coupling mechanisms at the core-mantle boundary, challenges to current inner core models, and the need for revised frequency scaling laws for Earth's anelastic response. The larger $\mathrm{Im}(K^{\mathrm{CMB}})$ values we observe are consistent with recent theoretical work by Rekier et al. (2025) on topographic coupling from shape-drag theory, suggesting electromagnetic coupling alone cannot fully explain the observed dissipation.

https://doi.org/10.5194/egusphere-2025-4428
Preprint. Discussion started: 30 September 2025

Our FCN free mode modeling reveals amplitude variations that show systematic differences from empirical models after 2000, highlighting remaining uncertainties in our understanding of FCN excitation processes. The halved Re(K^{ICB}) values, combined with recent seismic evidence for inner core deformation on annual timescales or for a mushy zone at the ICB, suggest that hydrostatic equilibrium assumptions in the nutation theory could require revision.

The updated BEP values provide refined constraints on Earth's deep interior structure and dynamics, but the persistent discrepancies between observations and theory across multiple parameters indicate that fundamental aspects of the nutation model may need revision. The larger coupling constants, altered compliances, and FCN amplitude differences collectively suggest that our current theoretical framework, while substantially improved since MHB 2000 in different parts, needs to be put together and thoroughly revised in terms of consistency as already highlighted by Ferrándiz et al. (2020).

These results will inform future Earth rotation modeling and contribute to our understanding of core-mantle and inner core boundary processes. The methodology presented here provide a robust computational framework for parameter estimation that can accommodate more sophisticated theoretical models. As our understanding of Earth's interior dynamics continues to evolve, future work should prioritize developing a unified nutation theory that integrates recent advances in core-mantle coupling mechanisms, inner core dynamics, and anelastic response models. Such a consistent theoretical framework is essential to reconcile the systematic parameter differences revealed by this expanded VLBI dataset and to fully exploit the growing precision of geodetic observations for Earth science applications.

Data availability. All CPO series used in this study can be obtained from the IVS product archive at the Crustal Dynamics Data Information System (CDDIS; Noll (2010)) at https://cddis.nasa.gov/archive/vlbi/ivsproducts/eops/. The International VLBI Service Nothnagel et al. (2017) coordinates the global VLBI components and resources that generate these data products.

Details of the empirical FCN model (Lambert, 2007) can be found in https://ivsopar.obspm.fr/fcn/. All constants used in the model can be found in the corresponding reference papers.

Author contributions. Y.C.: Methodology, Software, Formal analysis, Writing - original draft. V.D.: Conceptualization, Supervision, Funding acquisition. A.R.: Methodology, Supervision, Writing - review & editing. J.R.: Validation, Writing - review & editing. C.B.: Conceptualization, Writing - review & editing.

Competing interests. The authors declare there are no conflicts of interest for this manuscript.

Acknowledgements. The research leading to these results has received funding from the European Research Council (ERC) under the European Union's Horizon 2020 research and innovation program (GRACEFUL Synergy Grant agreement No 855677), as well as from the

https://doi.org/10.5194/egusphere-2025-4428
Preprint. Discussion started: 30 September 2025

Belgian National Fund for Scientific Research (NUTATION 2024 ERC-POC FNRS project No R.E001.26) following an ERC Seal of Excellence.

We thank S. Lambert for providing additional CPO series for validation purposes.

https://doi.org/10.5194/egusphere-2025-4428
Preprint. Discussion started: 30 September 2025

References

Aubert, J.: Flow throughout the Earth's core inverted from geomagnetic observations and numerical dynamo models, Geophysical Journal International, 192, 537–556, 2013.

Buffett, B., Mathews, P., and Herring, T.: Modeling of nutation and precession: effects of electromagnetic coupling, Journal of Geophysical Research: Solid Earth, 107, ETG–5, 2002.

Chao, B., Ray, R., Gipson, J., Egbert, G. D., and Ma, C.: Diurnal/semidiurnal polar motion excited by oceanic tidal angular momentum, Journal of Geophysical Research: Solid Earth, 101, 20 151–20 163, 1996.

Cheng, Y. and Bizouard, C.: Effect of the ocean tide on the Earth nutation: an updated assessment, Advances in Space Research, 2025.

Defraigne, P., Dehant, V., and Wahr, J. M.: Internal loading of an inhomogeneous compressible Earth with phase boundaries, Geophysical Journal International, 125, 173–192, 1996.

Dziewonski, A. M. and Anderson, D. L.: Preliminary reference Earth model, Physics of the earth and planetary interiors, 25, 297–356, 1981.

Ferrándiz, J. M., Gross, R. S., Escapa, A., Getino, J., Brzeziński, A., and Heinkelmann, R.: Report of the IAU/IAG joint working group on theory of Earth rotation and validation, in: Beyond 100: The Next Century in Geodesy: Proceedings of the IAG General Assembly, Montreal, Canada, July 8-18, 2019, pp. 99–106, Springer, 2020.

Herring, T., Mathews, P., and Buffett, B.: Modeling of nutation-precession: Very long baseline interferometry results, Journal of Geophysical Research: Solid Earth, 107, ETG–4, 2002.

Koot, L., Rivoldini, A., De Viron, O., and Dehant, V.: Estimation of Earth interior parameters from a Bayesian inversion of very long baseline interferometry nutation time series, Journal of Geophysical Research: Solid Earth, 113, 2008.

Lambert, S.: Empirical modeling of the retrograde Free Core Nutation, Technical Note, https://ivsopar.obspm.fr/fcn/notice.pdf, 2007.

Lobanov, S. S., Soubiran, F., Holtgrewe, N., Badro, J., Lin, J.-F., and Goncharov, A. F.: Contrasting opacity of bridgmanite and ferropericlase in the lowermost mantle: Implications to radiative and electrical conductivity, Earth and Planetary Science Letters, 562, 116 871, 2021.

Lyard, F. H., Allain, D. J., Cancet, M., Carrère, L., and Picot, N.: FES2014 global ocean tide atlas: design and performance, Ocean Science, 17, 615–649, 2021.

Mathews, P., Buffett, B. A., Herring, T. A., and Shapiro, I. I.: Forced nutations of the Earth: Influence of inner core dynamics: 1. Theory, Journal of Geophysical Research: Solid Earth, 96, 8219–8242, 1991.

Mathews, P. M., Herring, T. A., and Buffett, B. A.: Modeling of nutation and precession: New nutation series for nonrigid Earth and insights into the Earth's interior, Journal of Geophysical Research: Solid Earth, 107, ETG–3, 2002.

Niell, A. E.: Global mapping functions for the atmosphere delay at radio wavelengths, Journal of geophysical research: solid earth, 101, 3227–3246, 1996.

Noll, C. E.: The crustal dynamics data information system: A resource to support scientific analysis using space geodesy, Advances in Space Research, 45, 1421–1440, https://doi.org/10.1016/j.asr.2010.01.018, 2010.

Nothnagel, A., Artz, T., Behrend, D., and Malkin, Z.: International VLBI Service for Geodesy and Astrometry: delivering high-quality products and embarking on observations of the next generation, Journal of Geodesy, 91, 711–721, https://doi.org/10.1007/s00190-016-0950-5, 2017.

re3data.org: VMF Data Server, https://doi.org/10.17616/R3RD2H, editing status 2020-12-14; re3data.org - Registry of Research Data Repositories, 2020.

https://doi.org/10.5194/egusphere-2025-4428
Preprint. Discussion started: 30 September 2025

Rekier, J., Trian, S., Barik, A., Abdulah, D., and Kang, W.: Constraints on Earth's Core-Mantle boundary from nutation, arXiv preprint arXiv:2507.01671, 2025.

Souchay, J. and Kinoshita, H.: Corrections and new developments in rigid earth nutation theory. I. Lunisolar influence including indirect planetary effects., Astronomy and Astrophysics, v. 312, p. 1017-1030, 312, 1017–1030, 1996.

Souchay, J. and Kinoshita, H.: Corrections and new developments in rigid-Earth nutation theory. II. Influence of second-order geopotential and direct planetary effect., Astronomy and Astrophysics, v. 318, p. 639-652, 318, 639–652, 1997.

Souchay, J., Loysel, B., Kinoshita, H., and Folgueira, M.: Corrections and new developments in rigid earth nutation theory-III. Final tables" REN-2000" including crossed-nutation and spin-orbit coupling effects, Astronomy and Astrophysics Supplement Series, 135, 111–131, 1999.

Tian, D. and Wen, L.: Seismological evidence for a localized mushy zone at the Earth's inner core boundary, Nature communications, 8, 165, 2017.

Vidale, J. E., Wang, W., Wang, R., Pang, G., and Koper, K.: Annual-scale variability in both the rotation rate and near surface of Earth's inner core, Nature Geoscience, 18, 267–272, 2025.

Wang, W., Vidale, J. E., Pang, G., Koper, K. D., and Wang, R.: Inner core backtracking by seismic waveform change reversals, Nature, 631, 340–343, https://doi.org/10.1038/s41586-024-07536-4, 2024.

Yseboodt, M., de Viron, O., Chin, T. M., and Dehant, V.: Atmospheric excitation of the Earth's nutation: Comparison of different atmospheric models, Journal of Geophysical Research: Solid Earth, 107, ETG–2, 2002.

Zhu, P., Rivoldini, A., Koot, L., and Dehant, V.: Basic Earth's Parameters as estimated from VLBI observations, Geodesy and Geodynamics, 8, 427–432, 2017.